JACS
JOURNAL OF THE AMERICAN CHEMICAL SOCIETY

ARTICLE

pubs.acs.org/JACS

Activation of a Water-Soluble Resorcinarene Cavitand at the Water−Phosphocholine Micelle Interface

Sacha Javor and Julius Rebek, Jr.*

The Skaggs Institute for Chemical Biology and Department of Chemistry, The Scripps Research Institute, 10550 North Torrey Pines Road, La Jolla, California 92037, United States

Supporting Information

ABSTRACT: The host−guest properties of a water-soluble resorcinarene cavitand bearing four guanidines at the feet were investigated in water and dodecylphosphocholine (DPC) micelles by NMR spectroscopy. While the binding of different guests in water was generally modest, the formation of the caviplexes was significantly enhanced in the presence of micelles and reached affinities typically observed for organic solvents. The increase in binding free energies of up to 3.2 kcal mol^{-1} was determined to be enthalpic in origin and was attributed to the disruption of velcrand dimers and subsequent conformational reorganization of the receptor induced by the micelles that acted as hosts for the cavitand. In agreement with the NMR data, molecular dynamics simulations reproduced the spontaneous incorporation of the cavitand into the micelle and provided a detailed picture of the positioning of the receptor at the DPC−water interface.

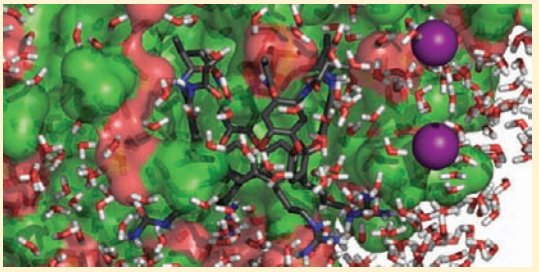

INTRODUCTION

Deep resorcinarene cavitands are versatile molecular hosts that can accommodate a variety of complementary molecular guests and temporarily isolate them from their environment.[1−4] Recently, several water-soluble cavitands[5] have been prepared by introducing various polar groups either at their rims[6−8] or at their feet.[9−12] In addition to their ability to bind suitable guests in aqueous solutions, cavitands also acted as hosts after being incorporated into micelles[13−15] and lipid bilayers,[16] suggesting their potential for biological applications.

In a therapeutic context, selective recognition and transmembrane transport of small polar molecules and ions are desirable capabilities for drug delivery vehicles.[17] The membrane translocation properties of a drug play a pivotal role in its pharmacokinetics. Because of the poor tissue accessibility, treatment of neurodegenerative diseases in particular remains a challenge for modern medicine.[18,19] Drug nanocarriers, especially those capable of shuttling across the blood brain barrier, could have major consequences for the treatment of several currently challenging disorders.[20] As an effort in that direction, we investigated the effect of dodecylphosphocholine (DPC) micelles on the behavior and the guest-binding capabilities of the water-soluble cavitand **1b**. Our finding is that the interaction between these membrane models and **1b**, rather than being detrimental, had a strong positive effect on the receptor's affinity.

The features of receptor cavitand **1b** (Scheme 1) comprise an electron-rich aromatic cavity suitable for guest recognition and an octaamide hydrogen-bonded "rim" that stabilizes the active "vase" conformation.[3] The relatively small cavity enables the binding of guests of an appropriate size only, ensuring a minimal interference with other biologically relevant molecules.[21]

Scheme 1. Synthesis of Receptor Cavitand 1b

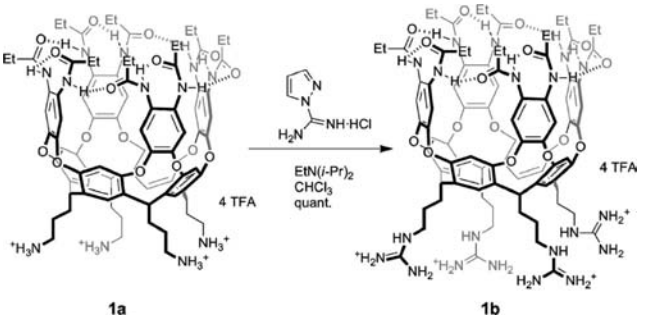

Drawing inspiration from cell penetrating peptides,[22] we introduced guanidinium[23] groups at the feet of the receptor. Recently, these same functionalities were introduced at the lower rim of structurally related calixarenes to produce remarkably effective cell transfection vectors.[24]

RESULTS AND DISCUSSION

Compound **1b** was prepared in 11 steps overall by guanidinylation of the previously described amino-footed cavitand **1a**[10] After RP-HPLC purification, it was obtained as the *tetrakis*-trifluoroacetate salt (Scheme 1). Cavitand **1b** was soluble up to 2.0 mM in D_2O and, in the absence of a soluble guest, adopted a nonbinding, C_{2v} or D_{2d} symmetric, "kite" conformation as evidenced by the characteristic ^{1}H NMR resonances.[25] Titration

Received: August 10, 2011
Published: September 12, 2011

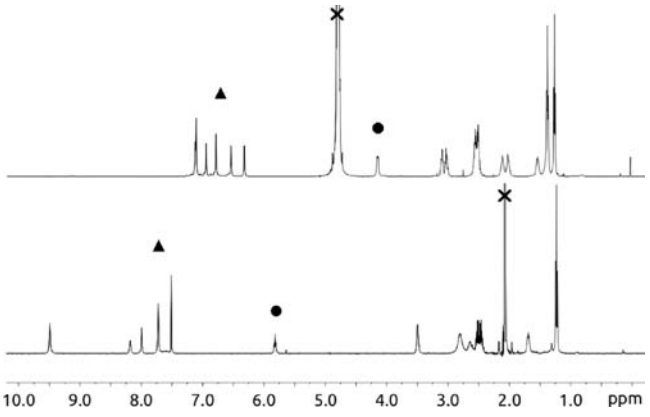

Figure 1. ^{1}H NMR spectra of cavitand **1b** (∼2.0 mM) in D_2O (top) and (∼10 mM) in acetone-d_6 (bottom). Aromatic (▲) and methine (●) resonances are characteristic for the "kite" (top) and "vase" (bottom) conformations. The solvent peak (×) is indicated.

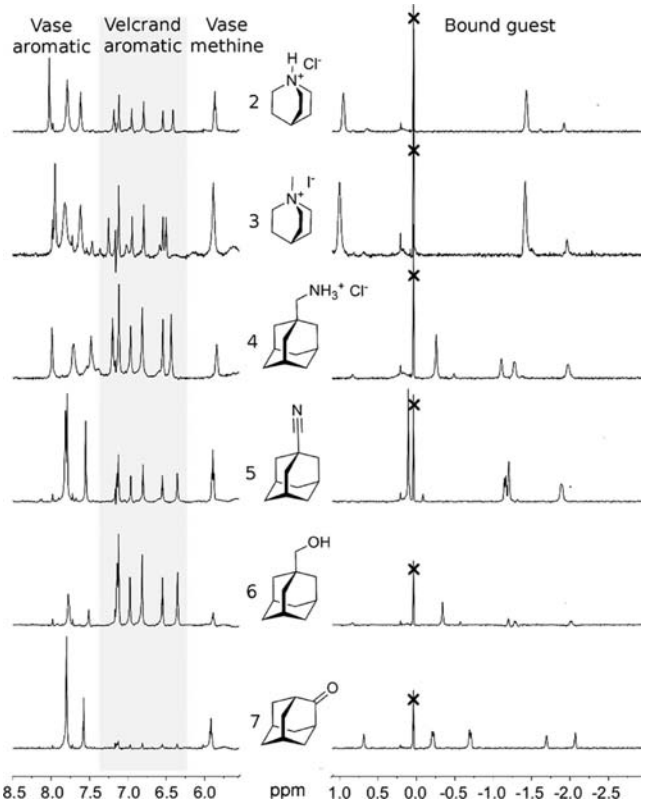

Figure 2. Aromatic and upfield regions of the ^{1}H NMR spectra for a variety of complexes of **1b**. Examples of caviplex formation illustrating the progressive kite-to-vase transition with increasing guest occupancy. [**1b**]:[guest] = 0.29:7.8, 0.16:9.4, 0.31:17, 0.26:0.52, 0.49:2.3, 0.24:3.2 mM. The resonances at 5.8 and >7.3 ppm correspond, respectively, to the methine and the aromatic protons of the caviplex in the vase conformation, and those upfield of zero correspond to its bound guest. The singlet at 0.04 ppm (×) is the external standard.

studies further confirmed a strong predominance of the dimeric (D_{2d}) "velcrand"[9,10,26] structure in D_2O (see the Supporting Information). For comparison, in acetone, **1b** adopted exclusively a monomeric, C_{4v} symmetric, "vase" conformation, suggesting that **1b** was able to respond to changes in its environment by significantly altering its conformation[10,27] (Figure 1).

Table 1. Association Constants and Corresponding Energies for the Formation of Caviplexes of 1b with Various Guests in D_2O at 300 K

	guest					
	2	**3**	**4**	**5**	**6**	**7**
K_a ($M^{-1/2}$)[a]	2.4	2.7	0.45	63	2.3	19
ΔG (kcal mol^{-1})	−0.52	−0.59	0.49	−2.5	−0.49	−1.8

[a] Calculated for the equilibrium $^1/_2$**1b**$_2$ + guest ⇆ guest⊂**1b** from the concentrations at equilibrium obtained by ^{1}H NMR signal integration relative to the reference signal. The total concentration of **1b** in solution was 0.14−0.31 mM. Whenever permitted by sufficient guest solubility, the values were obtained by titration, and the given values are the average of 3−8 data points.

Receptor **1b** formed (1:1) inclusion complexes with different cationic and neutral guests in D_2O at millimolar concentrations of guest. However, anionic guests, such as sulfonates and carboxylates, caused the precipitation of the cavitand at submillimolar concentrations, possibly by forming ion-pairs with the cationic feet. The formation of kinetically stable complexes was evidenced by the presence of guest resonances in the characteristic far upfield region of the NMR spectra. This is a well-established consequence of the large anisotropy imparted by the eight aromatic panels that define the cavity (Figure 2). At 300 K, **1b** adopted two distinct conformations in equilibrium: unbound velcrand[26] and guest-induced vase. The equilibrium between kite and induced vase has been recently described with cavitands bearing tetraethyleneglycols at the feet.[12] Interestingly, this behavior contrasted with that observed with the closely related amino-footed cavitand **1a** where some guests induced the vase conformation without necessarily producing a complex kinetically stable on the NMR time scale.[10]

Host−Guest Complexation in Water. In water, the guests oriented their polar functionalities near the solvent-accessible open end of the receptor and buried their most hydrophobic parts deep inside the host (Figure 2). Acetylcholine, which has a small hydrophobic portion, did not form a detectable complex with **1b** even at high (>20 mM) concentrations (see the Supporting Information). For the other guests investigated, the K_a values ranged between 0.45 and 63 $M^{-1/2}$ (Table 1). Similar values were reported for other octaamide resorcinarene cavitands in water.[10,12] As expected, the highest affinities were observed for the most hydrophobic guests in water, while the two polar adamantanes showed the poorest binding. The two quinuclidinium guests showed intermediate affinities, suggesting additional cation−π interactions in the complex.

The relatively modest binding energies for cavitands in water are the result of the preference to form velcrand dimers in protic solvents. These structures minimize the exposed hydrophobic surface but are incompatible with the binding of guests and need to be separated prior to the formation of the caviplex. The absence of the "unoccupied" vase conformer of **1b** suggested that this state was energetically highly disfavored in water (Figure 2). This observation was also supported by EXSY NMR.[28] The study of the dissociative process of the caviplex **2**⊂**1b** revealed a k_{-1} value of 2.32 ± 0.34 s^{-1} corresponding to a free energy of complex dissociation ($\Delta G^{\ddagger}$) of 17.1 ± 0.1 kcal mol^{-1} at 300 K[29] (see the Supporting Information). Similar values have been reported for other octaamide cavitands in water using such guests.[2,8,12,30]

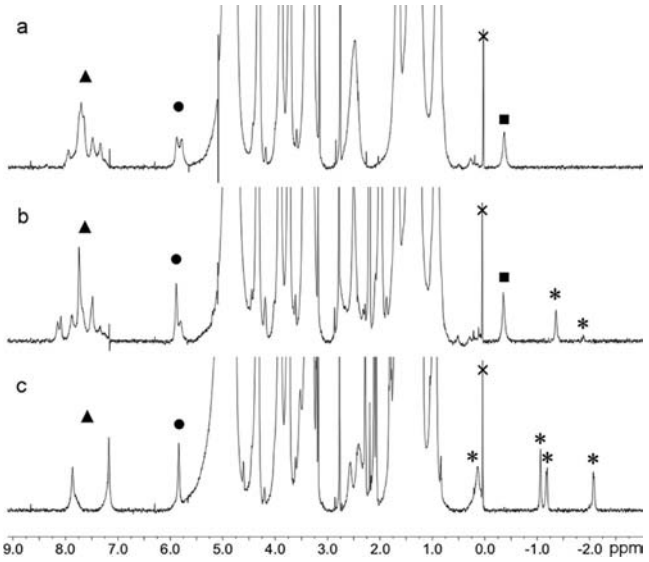

Figure 3. ^{1}H NMR spectra of **1b** in D_2O in the presence of 20 mM of DPC. (a) **1b** (0.4 mM) alone, (b) **1b** (0.3 mM) in the presence of **2** (7.5 mM), and (c) **1b** (0.3 mM) in the presence of **5** (0.6 mM). The singlet at 0.04 ppm (×) corresponds to the external standard. The aromatic (▲) and methine (●) resonances of **1b** as well as the bound trimethylammonium of DPC (■) and bound soluble guest (*) signals are indicated.

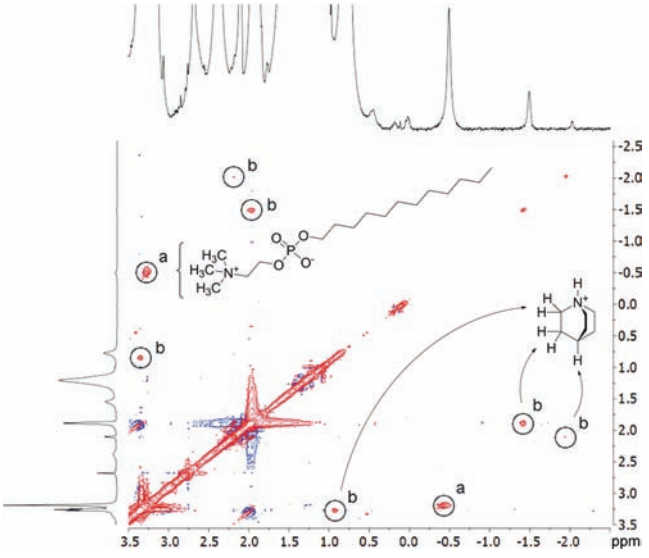

Figure 4. Upfield region of the ^{1}H ROESY spectrum of **1b** in the presence of DPC (20 mM) and **2**. The "a" indicates the exchange peak between the bound and unbound trimethylammonium of DPC, while "b" indicates the exchange peaks between the bound and free guest **2**.

Receptor 1b in the Presence of DPC Micelles. The behavior of **1b** in D_2O was dramatically altered in the presence of DPC micelles that were used to simulate biological membranes.[31] When 20 mM DPC was added, a concentration far above the critical micellar concentration (CMC = 1.1 mM),[32] in the absence of another soluble guest, the NMR spectrum of **1b** exhibited aromatic resonances exclusively downfield of 7.2 ppm as well as two methine resonances at 5.8 ppm: characteristic signals of the vase conformation (Figure 3a). The velcrand resonances observed in D_2O alone were absent from the spectrum, speaking for strong interactions between **1b** and the DPC micelles. In addition to the cavitand and micelle resonances, a broad upfield signal at −0.4 ppm was present in the NMR spectrum in the absence of added soluble guest (Figure 3a). ROESY experiments showed chemical exchange between this peak and the trimethylammonium resonance of DPC at 3.28 ppm (Figure 4). The presence of the polar head of the micelle inside **1b** therefore localized the cavitand near the micelle−water interface. The integration of this signal accounted for 2.3 protons corresponding to 25% of **1b** acting as a host for DPC while being itself the guest of the micelle. The simultaneous presence of occupied and empty vase conformer is consistent with multiple methine resonances observed in the absence of a guest.

Remarkably, **1b** recognized the polar head of DPC rather than its hydrophobic tail, in contrast to the behavior observed with all of the soluble guests (Figure 2).[12,14,15,33] The absence of any observable binding of DPC below the CMC suggested that neither its hydrophobic tail nor the phosphocholine head were sufficiently good guests in water (see the Supporting Information). The preorganized vase-like conformer of **1b**, observed exclusively above the CMC, apparently has an enhanced propensity to form caviplexes leading to trimethylammonium recognition. Perhaps the productive interaction between the micelle and **1b** involves positional constraints that require the receptor to be placed close to the surface of the micelle in the immediate vicinity of the phosphocholine functions. The choice of binding the polar end of the surfactant could be a consequence of the overall environment.

Molecular Dynamics. To test this hypothesis, the behavior of **1b** was simulated in the presence of a 65-molecule DPC micelle, in explicit solvent, using molecular dynamics (MD) with the GROMACS 4 package.[34] After manually placing **1b** in the vicinity of the micelle and adding the 11 920 solvent molecules and 4 chloride counterions, the system was simulated for 18 ns at 300 K. Multiple MD trajectories calculated starting from the same initial coordinates confirmed that the cavitand had the possibility to either interact with the micelle or diffuse away from it depending on the initial, randomly generated, atom velocities at 300 K, validating the starting point as an equilibrium position.

Salt bridges between guanidinium and phosphate groups have been widely studied and used for molecular recognition in various artificial systems.[35] The same interactions have also been proposed as an essential step in the peptide−membrane association that leads to the "arginine magic effect" observed with polyarginine peptides.[23,24] Our modeling suggested that they might contribute likewise to the recognition of DPC micelles by **1b**. Stable ion pairs between guanidiniums of **1b** and phosphates of DPC were formed very early in the MD trajectory (Figure 5A). Following these events, the progressive formation of additional interactions and the reorganization of the micelle surface to optimize hydrophobic contacts led to the gradual incorporation of the receptor into the micelle in approximately 2.5 ns (Figure 5B). It must be mentioned, however, that earlier reports of cavitands that do not possess guanidinium functions also enjoyed incorporation into micelles or lipid bilayers indicating the existence of alternative mechanisms.[13,14,16] After penetrating below its surface, the solvent-filled cavitand stabilized at ∼1.8 nm of the center of the micelle (Figure 5D). In this position, a significant portion of its hydrophobic surface is surrounded by the alkyl chains of DPC, while its open-end appears freely

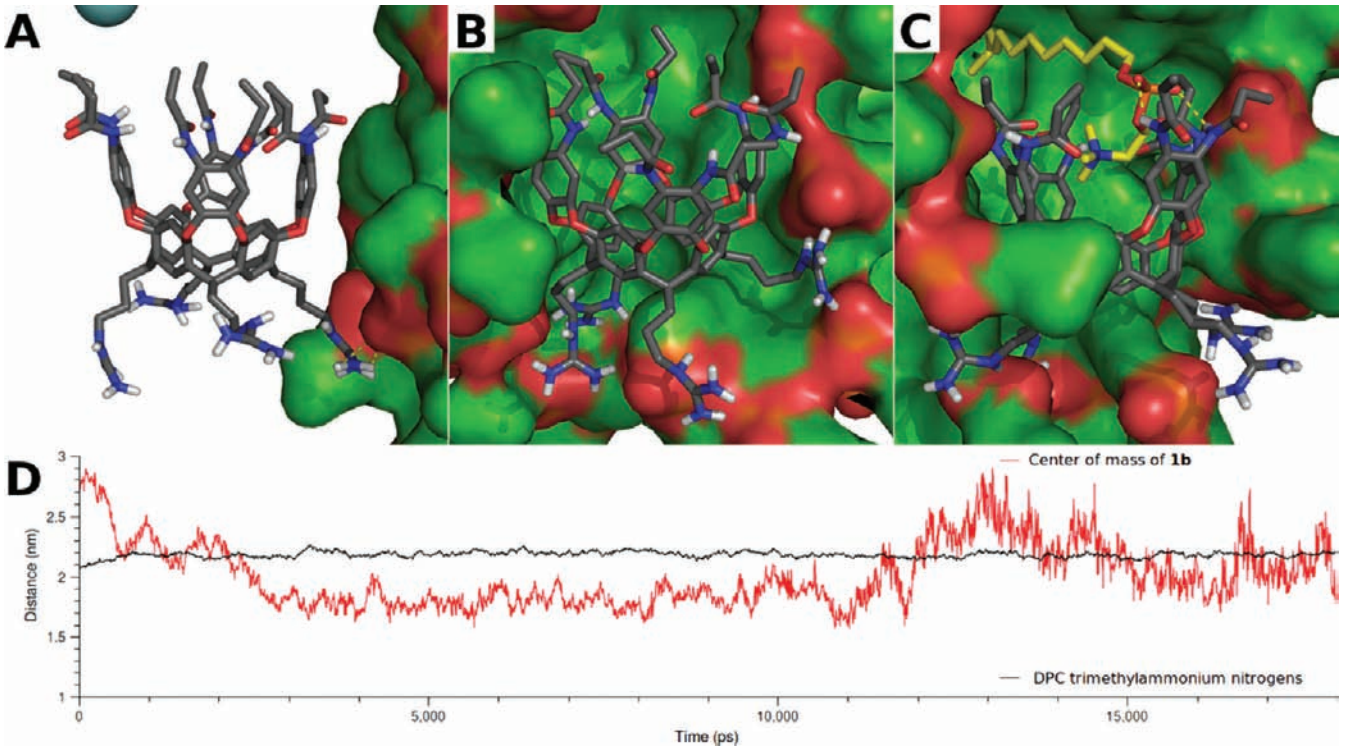

Figure 5. Molecular dynamics of **1b** (stick representation) in the presence of a 65-molecule DPC micelle (surface representation) in explicit H_2O at 300 K. (A) Snapshot of the trajectory after 99 ps showing early polar contacts (yellow dashed lines) between **1b** and DPC. (B) Conformation after 5 ns of the solvent-filled **1b** embedded in the micelle. (C) Snapshot after 17 ns of **1b** embedded in the micelle and binding a trimethylammonium group of one of the DPC molecules (Figures 3a, 4). Dashed yellow lines depict selected hydrogen bonds. Carbons are depicted in gray, green, and yellow, nitrogens in blue, oxygens in red, hydrogens in white, phosphorus in orange, and chloride in cyan. The solvent molecules were omitted for clarity. (D) Graph of the distance over time between the center of mass (COM) of the micelle and the COM of **1b** (red line). The average distance of the ammonium nitrogens of DPC and the COM of the micelle (black line) was used to define the position of the surface of the micelle.

Table 2. Association Constants and Corresponding Energies for the Formation of Caviplexes of 1b in D_2O in the Presence of DPC (20 mM)

	guest					
	2	**3**	**4**	**5**	**6**	**7**
K_a (M^{-1})[a]	31	52	11	2400	530	2300
ΔG (kcal mol^{-1})	−2.0	−2.4	−1.4	−4.6	−3.7	−4.6
$\Delta\Delta G$ (kcal mol^{-1})[b]	−1.5	−1.8	−1.9	−2.1	−3.2	−2.8

[a] Calculated for the equilibrium **1b** + guest ⇆ guest⊂**1b** at 300 K from the concentrations at equilibrium obtained by ^{1}H NMR signal integration relative to the reference signal. The total concentration of **1b** in solution was 0.18−0.45 mM. [b] $\Delta\Delta G = \Delta G_{D2O} - \Delta G_{DPC}$.

accessible from the bulk solvent (Figure 5B). This orientation, allowing the reversible binding of soluble guests, is consistent with the exchange of guest observed by ROESY NMR (Figure 4). Experimentally, the loss of symmetry associated with such positioning was supported by significant NMR signal broadening and increased number of vase resonances (Figure 3a). Other studies,[13] using uncharged cavitands, did not show reduced symmetry, suggesting that the amphiphilic nature of **1b** could be responsible for its placement at the water−micelle interface. The hydrophobic contacts with DPC presumably compete with the binding of another molecule of **1b** and attenuate the formation of velcrands at the micelle's surface. The system remained relatively stable in this configuration for approximately 7 ns. The water molecules, that were originally inside the cavitand, were then replaced with the trimethylammonium group of one the DPC molecules that constitute the micelle. At first, only a shallow binding was observed. After sampling different closely related conformations over several nanoseconds, the system adjusted by extracting the cavitand closer to the surface of the micelle (Figure 5D). This position allowed the ammonium to bind deep inside the cavity in excellent agreement with all of the NMR evidence (Figures 3 and 4). In this conformation, the MD also predicted possible hydrogen bonding between the amides of the rim of **1b** and the phosphate oxygens of DPC. The hydrophobic pocket formed by the micelle to accommodate **1b** (Figure 5B and C) could provide the local organic microenvironment that favors the vase conformation (Figure 1). A similar mechanism was invoked to describe the large conformational changes that characterize the "molecular umbrellas".[36,37] The fact that induction of the vase conformation was not observed when DPC was present at concentrations below its CMC supported the hypothesis that the change in conformation of **1b** follows a different mechanism than the guest-induced fit and requires the presence of fully formed micelles (see the Supporting Information).

Binding of Guests in the Presence of DPC. Cavitand **1b** formed complexes with the all of the guests **2**−**7** in the presence of DPC micelles.[38] At low concentrations of guests, upfield resonances for both bound guest and bound trimethylammonium

were observed in equilibrium (Figure 3b). The bound trimethylammonium was displaced in a concentration-dependent manner when a larger excess or a better guest was used (Figure 3c). In agreement with the observed vase geometry, titration experiments using **2** indicated that receptor **1b** behaved like a monomeric species in presence of micelles (see the Supporting Information). As a probable consequence of the conformational preorganization, the observed K_a values were significantly higher (up to a 230-fold increase for **6**) than the values observed in pure D_2O (Table 2). The values ranged from 1.1×10^1 to 2.4×10^3 M^{-1} corresponding to 1.5−3.2 kcal mol^{-1} of extra stabilization of the caviplexes. This range of values is typically observed with cavitands in organic solvents,[10,11,21,39] suggesting that **1b** experiences the micelle as an environment similar to bulk organic solvent. The strongest increases in binding (2.1−3.2 kcal mol^{-1}) were observed with the neutral guests. A slightly lower increase in binding of charged guests (1.5−1.9 kcal mol^{-1}) might be caused by the extraction of the guest's counterion into a less polar environment.

The van't Hoff plots for **2**⊂**1b** indicated that the binding of the guest was enthalpically favored with a small entropic penalty (see the Supporting Information). The ΔH values were −3.0 and −8.1 kcal mol^{-1} for the formation of the caviplex in D_2O and DPC micelles, respectively. Negative enthalpy values likely reflect the formation of the seam of hydrogen bonds and the cation−π interaction in the caviplex. The increase of $-\Delta H$ in the presence of DPC could be attributed to the preorganization of the receptor that allows the formation of the complex without the need to lose interactions in the velcrand dimer first. The small negative ΔS values, −8.4 and −19.7 cal K^{-1} mol^{-1} in water and DPC micelles, respectively, contrasted strongly with other cavitands in water where the formation of the complex was driven by a strong increase in entropy.[12] As compared to previously described cavitands, the NMR spectra of **1b** showed very sharp and well-resolved velcrand resonances. Positive ΔS values observed for other systems could be caused by the disruption of aggregated species that appear not to be present in the case of **1b**. A more negative entropy of formation in the presence of micelles is consistent with the reduction of the degrees of freedom in the micelle-bound complex.

CONCLUSIONS

In summary, we have shown that cavitand receptors increase their host−guest capabilities after being spontaneously incorporated into phosphocholine micelles. This property has consequences for the development of membrane transporters based on the deepened resorcinarene scaffold. Previous reports described the spontaneous incorporation of cavitands into diverse membrane models but always at the cost of lowering their affinity for the guests.[13−16] Rather than aiming for artificial membrane receptors that would retain some residual caviplex formation ability, it may be more useful to design environment-sensing receptors that become activated *in vivo* only under selected circumstances. Indeed, one earmark of membrane protein receptors is that they display the intended activity only when correctly embedded in the lipid bilayer. The exploitation of similar synergistic effects points the way to new classes of therapeutics where several programmable molecular recognition events could be multiplexed to achieve complex tasks on the molecular level.

EXPERIMENTAL SECTION

Instrumentation. ^1H, ^{13}C, 2D NOESY, ROESY, and HMQC NMR spectra were recorded on an Avance Bruker DRX-600 spectrometer with a 5 mm QNP probe or a 5 mm DCH cryoprobe. Deuterated NMR solvents were obtained from Cambridge Isotope Laboratories, Inc., Andover, MA, and used without further purification. Proton (^1H) chemical shifts are reported in parts per million (δ) with respect to tetramethylsilane (TMS, $\delta = 0$) and are referenced internally with respect to the residual solvent proton impurity. MALDI TOF spectra were recorded on an Applied Biosystems Voyager STR mass spectrometer. RP-HPLC purifications were performed using a Waters XBridge BEH 130 Prep C18 10 μm column (19 × 250 mm) mounted on a Waters preparative system.

Synthesis of Cavitand 1b. A solution of tetraamine footed cavitand[10] **1a** (42 mg, 0.021 mmol) and 1-*H*-pyrazole-1-carboxamidine hydrochloride (16 mg, 0.10 mmol, 5.0 equiv) in chloroform (9.8 mL) and diisopropylethylamine (0.50 mL) was stirred at 50 °C for 16 h. The solvents were evaporated. The residue was purified by RP-HPLC and lyophilized to yield cavitand **1b** (44 mg, 97%) as a colorless fluffy solid. ^1H NMR (600 MHz, acetone-d_6) δ = 9.47 (s, 8H), 8.16 (s, 4H), 7.98 (s, 4H), 7.71 (s, 8H), 7.49 (s, 4H), 5.80 (t, J = 9.0 Hz, 4H), 3.55−3.4 (m, 8H), 2.79 (br s, 16H), 2.7−2.55 (m, 8H), 2.55−2.4 (m sym, 16H), 1.7−1.6 (m, 8H), 1.21 (t, J = 7.9 Hz, 24H). ^{13}C NMR (150 MHz, acetone-d_6) δ = 174.41, 158.93, 155.82, 150.32, 136.73, 129.58, 126.13, 121.80, 117.20, 42.13, 34.77, 31.35, 29.91, 28.99, 10.67. MALDI-TOF-MS: m/z calcd for $C_{92}H_{109}N_{20}O_{16}$ $[M + H]^+$, 1749.8; found, 1750.

Determination of Concentrations in Solution. A sealed capillary containing a solution of sodium 3-(trimethylsilyl)-propionate-2,2,3,3-d_4 at an apparent concentration of 44.6 μM in D_2O (calibrated by NMR) present in the NMR tube was used as external standard for the determination of concentrations in solution. All of the concentrations were determined by integration of ^1H NMR signals relative to the trimethylsilane reference.

Determination of Association Constants. The association constants were calculated from the concentrations of different species in solution by directly substituting their values into the corresponding equilibrium constant equations.

2D NMR. The 2D NOESY and ROESY spectra of the cavitands were recorded at 300 K at 600 MHz with the phase-sensitive NOESY and ROESY pulse sequences supplied with the Bruker Topspin software. Each of the 512 F1 increments was accumulated for 32 or 48 scans for NOESY or ROESY experiments, respectively. For EXSY, two NOESY spectra were taken sequentially, one with 300 ms mixing time and then with 0 ms mixing time. The caviplex dissociation rate constant k_{-1} was calculated using the EXSYCALC (Mestrelab) program[28] and converted to $\Delta G^{\ddagger}$ using the Eyring−Polanyi equation.

Modeling. The starting conformation and the partial charges of the monomeric **1b** were obtained by optimization of the geometry using the semiempirical PM3 method in the Spartan '04 software and converted to GROMOS (gmx53a6 force field) topology using the Topolbuild 1.3 program. The DPC molecules were parametrized in agreement with the Berger lipid implementation,[40] and the starting conformation for the DPC micelle was taken from a minimized structure described elsewhere.[41] Receptor **1b** was placed by hand in the proximity of the micelle at a distance corresponding to approximately one cavitand size using the PyMOL software.[42] The combined model was then centered in a 395 nm^3 dodecahedral periodic box that was subsequently filled with 11 920 water molecules (SPCE model) and 4 chloride counterions. The energy of the whole system was minimized, and a 50 ps position restrained MD was used to soak the solute molecules with the solvent and produce the starting conformation used in the MD study. The simulation was performed in an NPT ensemble at 300 K and 1 bar for 18 ns with a step size of 2 fs. The trajectory was recorded every picosecond and used for subsequent analysis.

■ ASSOCIATED CONTENT

Supporting Information. Experimental procedures, ^{1}H, ^{13}C, NOESY, ROESY, and HMQC NMR spectra, NMR titration experiments, details of the modeling procedures, and files. This material is available free of charge via the Internet at http://pubs.acs.org.

■ AUTHOR INFORMATION

Corresponding Author
jrebek@scripps.edu

■ ACKNOWLEDGMENT

We are grateful to the Skaggs Institute for Research and the United States Department of Defense, Defense Threat Reduction Agency for financial support. S.J. is a Skaggs Postdoctoral Fellow and was supported by the Swiss National Science Foundation (SNF). We also thank Dr. Daniel Ryan and Dr. Eric Busseron for helpful discussions during the research and suggestions concerning this manuscript.

■ REFERENCES

(1) Moran, J. R.; Karbach, S.; Cram, D. J. *J. Am. Chem. Soc.* **1982**, *104*, 5826–5828.
(2) Rudkevich, D. M.; Hilmersson, G.; Rebek, J., Jr. *J. Am. Chem. Soc.* **1997**, *119*, 9911–9912.
(3) Rudkevich, D. M.; Hilmersson, G.; Rebek, J., Jr. *J. Am. Chem. Soc.* **1998**, *120*, 12216–12225.
(4) Högberg, A. G. S. *J. Am. Chem. Soc.* **1980**, *102*, 6046–6050.
(5) Biros, S. M.; Rebek, J., Jr. *Chem. Soc. Rev.* **2007**, *36*, 93–104.
(6) Hof, F.; Trembleau, L.; Ullrich, E. C.; Rebek, J., Jr. *Angew. Chem., Int. Ed.* **2003**, *42*, 3150–3153.
(7) Biros, S. M.; Ullrich, E. C.; Hof, F.; Trembleau, L.; Rebek, J., Jr. *J. Am. Chem. Soc.* **2004**, *126*, 2870–2876.
(8) Hooley, R. J.; Van Anda, H. J.; Rebek, J., Jr. *J. Am. Chem. Soc.* **2006**, *128*, 3894–3895.
(9) Haino, T.; Rudkevich, D. M.; Rebek, J., Jr. *J. Am. Chem. Soc.* **1999**, *121*, 11253–11254.
(10) Haino, T.; Rudkevich, D. M.; Shivanyuk, A.; Rissanen, K.; Rebek, J., Jr. *Chem.-Eur. J.* **2000**, *6*, 3793–3805.
(11) Butterfield, S. M.; Rebek, J., Jr. *J. Am. Chem. Soc.* **2006**, *128*, 15366–15367.
(12) Lledó, A.; Rebek, J., Jr. *Chem. Commun.* **2010**, *46*, 8630–8632.
(13) Schramm, M. P.; Hooley, R. J.; Rebek, J., Jr. *J. Am. Chem. Soc.* **2007**, *129*, 9773–9779.
(14) Trembleau, L.; Rebek, J., Jr. *Chem. Commun.* **2004**, 58–59.
(15) Kim, Y. J.; Lek, M. T.; Schramm, M. P. *Chem. Commun.* **2011**, *47*, 9636–9638.
(16) Liu, Y.; Liao, P.; Cheng, Q.; Hooley, R. J. *J. Am. Chem. Soc.* **2010**, *132*, 10383–10390.
(17) Torchilin, V. P. *Adv. Drug Delivery Rev.* **2006**, *58*, 1532–1555.
(18) Cotzias, G. *N. Engl. J. Med.* **1968**, *287*, 630–630.
(19) (a) Rosenberg, G. S.; Davis, K. L. *Am. J. Clin. Nutr.* **1982**, *36*, 709–720. (b) Bazalakova, M. H.; Blakely, R. D. *Handb. Exp. Pharmacol.* **2006**, *175*, 525–544.
(20) Bhaskar, S.; Tian, F.; Stoeger, T.; Kreyling, W.; de la Fuente, J. M.; Grazú, V.; Borm, P.; Estrada, G.; Ntziachristos, V.; Razansky, D. *Part. Fibre Toxicol.* **2010**, *7*, 3.
(21) Lledó, A.; Hooley, R. J.; Rebek, J., Jr. *Org. Lett.* **2008**, *10*, 3669–3671.
(22) (a) Frankel, A. D.; Pabo, C. O. *Cell* **1988**, *55*, 1189–1193. (b) Plénat, T.; Deshayes, S.; Boichot, S.; Milhiet, P. E.; Cole, R. B.; Heitz, F.; Le Grimellec, C. *Langmuir* **2004**, *20*, 9255–9261. (c) Deshayes, S.; Plénat, T.; Aldran-Herrada, G.; Divita, G.; Le Grimellec, C.; Heitz, F. *Biochemistry* **2004**, *43*, 7698–7706.
(23) (a) Nishihara, M.; Perret, F.; Takeuchi, T.; Futaki, S.; Lazar, A. N.; Coleman, A. W.; Sakai, N.; Matile, S. *Org. Biomol. Chem.* **2005**, *3*, 1659–1669. (b) Sakai, N.; Matile, S. *J. Am. Chem. Soc.* **2003**, *125*, 14348–14356.
(24) (a) Bagnacani, V.; Sansone, F.; Donofrio, G.; Baldini, L.; Casnati, A.; Ungaro, R. *Org. Lett.* **2008**, *10*, 3953–3956. (b) Sansone, F.; Dudič, M.; Donofrio, G.; Rivetti, C.; Baldini, L.; Casnati, A.; Cellai, S.; Ungaro, R. *J. Am. Chem. Soc.* **2006**, *128*, 14528–14536.
(25) The methine C−H resonances at 4.15 ppm and aromatic C−H resonances below 7.3 ppm are characteristic of the "kite" conformation. Additionally, the observed splitting of the signals, including the aliphatic, is a consequence of the 2-fold symmetry of this conformation. Alternatively, the 4-fold symmetrical "vase" conformation is characterized by aromatic C−H resonances that are usually downfield of 7.2 and displays a characteristic methine C−H signal at 5.8 ppm.
(26) Cram, D. J.; Choi, H. J.; Bryant, J. A.; Knobler, C. B. *J. Am. Chem. Soc.* **1992**, *114*, 7748–7765.
(27) **1b** was soluble at 55 mM in acetone. When the TFA counterions were replaced by chlorides, the cavitand was insoluble in acetone but retained 1.9 mM solubility in D_2O.
(28) (a) Perrin, C. L.; Dwyer, T. J. *Chem. Rev.* **1990**, *90*, 935–967. (b) Zolnai, Z.; Juranić, N.; Vikić-Topić, D.; Macura, S. *J. Chem. Inf. Comput. Sci.* **2000**, *40*, 611–621.
(29) The EXSY experiment was performed with mixing time 300 ms, [**1**] = 0.23 mM, [**2**] = 5.6 mM at 300 K.
(30) Hooley, R. J.; Shenoy, S. R.; Rebek, J., Jr. *Org. Lett.* **2008**, *10*, 5397–5400.
(31) Cansell, M.; Gouygou, J. P.; Jozefonvicz, J.; Letourneur, D. *Lipids* **1997**, *32*, 39–44.
(32) Stafford, R. E.; Fanni, T.; Dennis, E. A. *Biochemistry* **1989**, *28*, 5113–5120.
(33) Trembleau, L.; Rebek, J., Jr. *Science* **2003**, *301*, 1219–1220.
(34) Hess, B.; Kutzner, C.; van der Spoel, D.; Lindahl, E. *J. Chem. Theory Comput.* **2008**, *4*, 435–447.
(35) (a) Schug, K. A.; Lindner, W. *Chem. Rev.* **2005**, *105*, 67–113. (b) Schmidtchen, F. P.; Berger, M. *Chem. Rev.* **1997**, *97*, 1609–1646.
(36) Mehiri, M.; Chen, W.-H.; Janout, V.; Regen, S. L. *J. Am. Chem. Soc.* **2009**, *131*, 1338–1339.
(37) Janout, V.; Regen, S. L. *Bioconjugate Chem.* **2009**, *20*, 183–192.
(38) With the exception of **6**, the guests were oriented in the same relative orientation as in D_2O alone (see the Supporting Information).
(39) Lledó, A.; Rebek, J., Jr. *Chem. Commun.* **2010**, *46*, 1637–1639.
(40) Berger, O.; Edholm, O.; Jähnig, F. *Biophys. J.* **1997**, *72*, 2002–2013.
(41) Tieleman, D. P.; van der Spoel, D.; Berendsen, H. J. C. *J. Phys. Chem. B* **2000**, *104*, 6380–6388.
(42) The PyMOL Molecular Graphics System, Version 1.2 r2, Schrödinger, LLC.